

# Study of Bose-Einstein Condensates by Means of Inverse Scattering Theory

report on the OTKA Project Nr IN 67371

performed at TU Budapest between 2007-2008

## Principal Investigator:

Barnabas Apagyí, Department of Theoretical Physics,  
Budapest University of Technology and Economics, Budapest

## Advisor:

Werner Scheid, Institute of Theoretical Physics, Justus-Liebig-University, Giessen

## Participant:

Enikő Regős, Department of Theoretical Physics,  
Budapest University of Technology and Economics, Budapest  
Present address: CERN LHC, Switzerland

## 1. Aims

This research proposal was an international extension of the research project Nr. T047035. The main aim of our research was the exploration of the stable solutions for two-component Bose-Einstein condensates by considering direct and inverse scattering methods. First, we wanted to investigate the Cox-Thompson fixed energy inverse scattering method and then, to apply it to an inversion of phase shifts obtained from an analysis of collision of Bose-Einstein condensates. From these investigations several papers have been published in journals of high international reputation.

Another aim was to directly simulate the Bose-Einstein condensate by solving the non-linear Schrödinger equation with an external potential trapping the condensate. This task has been accomplished by a careful and intensive work which first starts with an one-component Bose-Einstein condensate. We have written and tested a numerical FORTRAN code which reproduces various analytic solutions of the problem, mainly in terms of different types of solitons. Then the code has been developed to the coupled two-component case, and also numerically tested for the example of coupled solitons which have an analytically known solution. Now we are planning to apply this code in different situations corresponding to various experimental possibilities. We want to study a stability analysis and to explore the parameter domain which is mostly suited to the experimental

situation of the creation of two-component Bose-Einstein condensates.

## 2. Summary

Bose-Einstein condensates have been investigated by means of direct and inverse scattering methods. A fixed-energy inverse scattering method has been developed, based on an earlier suggestion by Cox and Thompson, for treating long and short ranged potentials. Simplified semi-analytic solutions have been given for the inverse scattering problem for cases when only even or odd partial waves contribute to the scattering amplitude. The result has been applied to invert experimental phase shifts obtained from the analysis of collisions of two Bose-Einstein condensates, each consisting of Rb-atoms. A condition has been given for the derivation of non-singular inverse potential. We have developed computer codes which simulate the time development of one- and two-component Bose-Einstein condensates. The codes have been tested numerically for the analytic example of coupled solitons. The coupled channel code may help in realising two-component Bose-Einstein condensates.

## 3. Report on the main results

### 3.1 Condition for obtaining non-singular potentials by using the Cox-Thompson inversion method

In this chapter we establish a condition for obtaining non-singular potentials using the Cox-Thompson inverse scattering method with one phase shift. The anomalous singularities of the potentials are avoided by maintaining unique solutions of the underlying Regge-Newton integral equation for the transformation kernel.

The Regge-Newton integral equation of the Cox-Thompson method (J. Cox and K. Thompson, J. Math. Phys. **11**, 805, (1970)) for the transformation kernel reads as

$$K(x, y) = g(x, y) - \int_0^x dt t^{-2} K(x, t) g(t, y), \quad x \geq y, \quad (1)$$

with the input symmetrical kernel defined as

$$g(x, y) = \sum_{l \in S} \gamma_l u_l(x_{<}) v_l(x_{>}), \quad \left\{ \begin{array}{c} x_{<} \\ x_{>} \end{array} \right\} = \left\{ \begin{array}{c} \min \\ \max \end{array} \right\} (x, y). \quad (2)$$

Here  $u_l$  and  $v_l$  means, respectively, the regular and irregular Riccati-Bessel functions defined as  $u_l(x) = \sqrt{\frac{\pi x}{2}} J_{l+\frac{1}{2}}(x)$ ,  $v_l(x) = \sqrt{\frac{\pi x}{2}} Y_{l+\frac{1}{2}}(x)$ , ( $J_{l+\frac{1}{2}}$

and  $Y_{l+\frac{1}{2}}$  are the Bessel functions ) and the explicit expression holds for the  $\gamma_l$  numbers:

$$\gamma_l = \frac{\prod_{L \in T} [l(l+1) - L(L+1)]}{\prod_{l' \in S, l' \neq l} [l(l+1) - l'(l'+1)]}, \quad l \in S, \quad (3)$$

with  $|S| = |T| < \infty$ ,  $T \subset (-1/2, \infty)$ ,  $S \subset (-1/2, \infty)$  and  $S \cap T = \emptyset$ . Let  $\Omega$  denote the set of zeros of the determinant

$$D(x) = \det(C), \quad [C]_{lL} = \frac{u_L(x)v'_l(x) - u'_L(x)v_l(x)}{l(l+1) - L(L+1)} \quad \forall x. \quad (4)$$

In Ref. (J. Cox and K. Thompson, J. Math. Phys. **11**, 815, (1970)) it is proved that this equation is uniquely solvable for  $x \in \mathbb{R}^+ \setminus \Omega$  and the elements of  $\Omega$  are isolated points. Therefore, the continuous solution of equation (1) (if it exists) is unique.

In Ref. (K. Chadan and P. C. Sabatier, *Inverse Problems in Quantum Scattering Theory* (Springer, New York, 1977), pp. 187-188.) it has been shown that the first moment of the potential  $tq(t)$  is not integrable near  $\tilde{x} \in \Omega$ . Therefore the potential  $q(x) := -\frac{2}{x} \frac{d}{dx} \frac{K(x,x)}{x}$  corresponding to the Schrödinger equation has poles of order (at least) 2 at these isolated points  $\tilde{x}$ . Such potentials are not in  $L_{1,1}(0, \infty)$  and we call them singular potentials.

To get non-singular potentials by the Cox-Thompson method is thus in an intimate connection with the uniqueness of solution of equation (1). In the one-term limit, the numerator of equation (4) becomes the Wronskian

$$W_{Ll}(x) = \frac{\pi x}{2} \left( J_{L+\frac{1}{2}}(x) Y'_{l+\frac{1}{2}}(x) - J'_{L+\frac{1}{2}}(x) Y_{l+\frac{1}{2}}(x) \right).$$

To ensure a unique solution of the Regge-Newton integral equation (1), we shall establish a condition for  $W_{Ll}(x) \neq 0$ ,  $x \in (0, \infty)$ . This is also the condition for constructing a non-singular potential  $q(x)$ ,  $x \in (0, \infty)$  at the one-term level  $|S| = |T| = 1$ .

Let  $S = \{l\}$  and  $T = \{L\}$ ,  $L \neq l$ . In order to get a potential that belongs to the class  $L_{1,1}(0, \infty)$  we proved the next statement.

**Theorem 0.1.**  $W_{Ll}(x) \neq 0$ ,  $x \in (0, \infty) \iff 0 < |L - l| \leq 1$ .

*Proof.* First we prove that there exists  $x > 0$  such that  $W_{Ll}(x) = 0$  if  $|L - l| > 1$ . Let  $1 + 4k < l - L < 3 + 4k$  with  $k \in \mathbb{Z}$ . Then the different

signs of the Wronskian at the origin

$$W_{Ll}(x \rightarrow 0) = x^{L-l} \left[ \frac{2^{l-L-1}(L+l+1)\Gamma(l+\frac{1}{2})}{\Gamma(L+\frac{3}{2})} + O(x^{2l+1}) \right] > 0$$

and at the infinity  $W_{Ll}(x \rightarrow \infty) = \cos \left[ (l-L) \frac{\pi}{2} \right] < 0$  clearly signal the existence of at least one zero position  $\tilde{x}$  for which  $W_{Ll}(\tilde{x}) = 0$  because of the continuity of  $W_{Ll}(x)$ .

For the uncovered region of  $3+4k < l-L < 5+4k$  with  $k \in \mathbb{Z} \setminus \{-1\}$  we shall use the standard notation for the  $n$ th zeros  $j_{L+\frac{1}{2},n}$ ,  $j'_{L+\frac{1}{2},n}$ ,  $y_{l+\frac{1}{2},n}$ ,  $y'_{l+\frac{1}{2},n}$  of the Bessel functions  $J_{L+\frac{1}{2}}(x)$ ,  $J'_{L+\frac{1}{2}}(x)$ ,  $Y_{l+\frac{1}{2}}(x)$ ,  $Y'_{l+\frac{1}{2}}(x)$ . Let now  $l < L$ . We term *regular* sequence of zeros if the following interlacing holds for the  $n$ th and  $(n+1)$ th zeros:  $y_{l+\frac{1}{2},n} < j_{L+\frac{1}{2},n} < y_{l+\frac{1}{2},n+1} < j_{L+\frac{1}{2},n+1}$ . It is a simple matter to see that the local extrema of  $W_{Ll}(x)$  within the interval  $y_{l+\frac{1}{2},n} < x < j_{L+\frac{1}{2},n+1}$  possess the same sign in case of a regular sequence interlacing. This is because at the extremum positions  $y_{l+\frac{1}{2},n}$  and  $j_{L+\frac{1}{2},n}$  of  $W_{Ll}(x)$  the Wronskian simplifies to

$$W_{Ll}(x_n) = \begin{cases} \frac{\pi x}{2} J_{L+\frac{1}{2}}(x_n) Y'_{l+\frac{1}{2}}(x_n) & \text{if } Y_{l+\frac{1}{2}}(x_n) = 0, x_n = y_{l+\frac{1}{2},n} \\ -\frac{\pi x}{2} J'_{L+\frac{1}{2}}(x_n) Y_{l+\frac{1}{2}}(x_n) & \text{if } J_{L+\frac{1}{2}}(x_n) = 0, x_n = j_{L+\frac{1}{2},n}. \end{cases}$$

Now, in case of any deviation from this regular sequence, e.g., when an *irregular* sequence  $y_{l+\frac{1}{2},n} < y_{l+\frac{1}{2},n+1} < j_{L+\frac{1}{2},n}$  is first encountered at a particular  $n = 1, 2, \dots$ , one gets different signs for the two consecutive extrema of the Wronskian at  $y_{l+\frac{1}{2},n}$  and  $y_{l+\frac{1}{2},n+1}$ , respectively. This assumes the appearance of a zero position of  $W_{Ll}(x)$  within the region  $y_{l+\frac{1}{2},n} < x < y_{l+\frac{1}{2},n+1}$ . In summary, observing regular sequences of interlacing for all  $n > 0$  is equivalent to the absence of roots of  $W_{Ll}(x)$ . To see that in the considered region such deviation from the regular sequence interlacing happens, we present the following argument. Let  $L' < L$  such that  $1+4k < l-L' < 3+4k$ . For  $W_{L'l}$  the first deviation from the regular sequence takes place at some  $n'$ . It is easy to see that by increasing  $L'$  to  $L$  one cannot get a regular sequence and the first deviation will occur at some  $n \leq n'$ . Note that the case  $L < l$  can be similarly treated.

Turning now to the most interesting domain of  $0 < |L-l| \leq 1$ , we consider again the case  $l < L$  and the regular sequence of zero interlacing,  $y_{l+\frac{1}{2},n} < j_{L+\frac{1}{2},n} < y_{l+\frac{1}{2},n+1} < j_{L+\frac{1}{2},n+1}$ . As indicated above, its fulfillment ensures the lack of a root of the Wronskian:  $W_{Ll}(x) \neq$

0,  $x \in (0 < x < \infty)$ . By noting that any  $n$ th zero of a Bessel function is a strictly growing function of the order it is sufficient to prove that  $y_{k,n} < j_{k+1,n} < y_{k,n+1} < j_{k+1,n+1}$ , holds for  $k \in (0, \infty)$  and  $n \in \mathbb{N} \setminus \{0\}$ . The only unknown inequality here is that of  $j_{k+1,n} < y_{k,n+1}$ . To prove its validity we use the known intermediate relation  $j'_{k,n+1} < y_{k,n+1}$ . Therefore, proving  $j_{k+1,n} < j'_{k,n+1}$  will be sufficient. Consider the known relation  $J_{k+1}(j'_{k,n+1}) = \frac{k}{j'_{k,n+1}} J_k(j'_{k,n+1})$  which means that  $J_{k+1}$  and  $J_k$  have the same sign at  $x = j'_{k,n+1}$ . Now because of the interlacing property  $j_{k,1} < j_{k+1,1} < j_{k,2} < \dots$  and the limit  $J_k(x \rightarrow 0) = 0^+ \forall k > 0$ , this implies that the  $n$ th zero of  $J_{k+1}(x)$  precedes the  $(n+1)$ th zero of  $J'_k(x)$ , i.e.  $j_{k+1,n} < j'_{k,n+1} < y_{k,n+1}$  which had to be proven. Note that the case  $L < l$  can be similarly treated.  $\square$

**Corollary 0.2.** *In case of  $|S| = 1$ , the Cox-Thompson inverse scattering scheme yields a potential of the class  $L_{1,1}(0, \infty)$  iff the condition  $0 < |l - L| \leq 1$  holds.*

In the course of the proof we obtained the following result of its own right:

**Proposition 0.3.** *Denoting the  $n$ th root of the Bessel functions  $J_\nu(x)$ ,  $Y_\nu(x)$ ,  $J'_\nu(x)$ , respectively, by  $j_{\nu,n}$ ,  $y_{\nu,n}$ ,  $j'_{\nu,n}$  then the following inequality is valid for  $\nu > 0$ :  $j_{\nu+1,n} < j'_{\nu,n+1}$ .*

This proposition adds two new inequality sequences to the known ones (see e.g. M. Abramowitz and I. A. Stegun, *Handbook of Mathematical Functions* (Dover Publications, New York, 1972), pp. 360-371.):  $j_{\nu,n} < j_{\nu+1,n} < j'_{\nu,n+1} < j_{\nu,n+1}$ , and  $j_{\nu+1,n} < y_{\nu,n+1}$ .

One can construct a potential that possesses one specified phase shift  $\delta_l$  ( $|S| = 1$ ) by using the inversion scheme of Cox and Thompson (see: B. Apagy, Z. Harman and W. Scheid, *J. Phys. A: Math. Gen.* **36**, 4815, (2003))

$$q(x) = -\frac{2}{x} \frac{d}{dx} \frac{K(x, x)}{x},$$

$$K(x, y) = \frac{l(l+1) - L(L+1)}{u_L(x)v'_l(x) - u'_L(x)v_l(x)} v_l(x)u_L(y),$$

$$\tan(\delta_l - l\pi/2) = \tan(-L\pi/2).$$

The last relation gives  $L = l - \frac{2}{\pi}\delta_l + 2n$ ,  $n \in \mathbb{Z}$ . For  $\delta_l \in [-\frac{\pi}{2}, \frac{\pi}{2}]$  Corollary 0.2 results in the choice of  $n = 0$ . Therefore, for any  $\delta_l$ , there is only one,

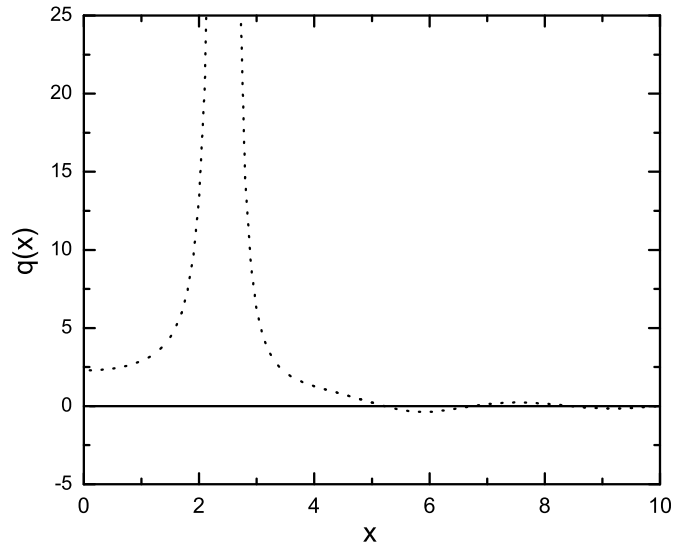


Figure 1: Non-singular (full line) and singular (dotted line) potentials yielded by  $\delta_l = 0$  and  $L \rightarrow 0$ , and  $L = 2$ .

easily identifiable non-singular potential and an infinite number of singular potentials that the Cox-Thompson method can produce.

For an example let us choose  $l = 0$  and  $\delta_0 = 0$ . In this case  $L = 2n$ ,  $n \in \mathbb{Z}$ .  $L = 0$  ( $n = 0$ ) is not permitted by the assumption  $S \cap T = \emptyset$ , however in order to get a non-singular potential one may replace this  $L = 0$  by  $L_n$  with  $\lim_{n \rightarrow \infty} L_n = 0$ . One gets at  $l = 0$ ,  $L = L_n$  and

$$K_n(x, x) = \frac{-L_n(L_n + 1)}{1 + \varepsilon_n^1} (v_0(x)u_0(x) + \varepsilon_n^2).$$

Since  $u_L(x)v_l'(x) - u_l'(x)v_L(x)$  and  $v_l(x)u_L(x)$  are continuous in  $L$  and  $u_l(x)v_l'(x) - u_l'(x)v_l(x) = 1$ ,  $\forall l$ ,  $\lim_{n \rightarrow \infty} \varepsilon_n^{1,2} = 0$  holds. Thus  $\lim_{n \rightarrow \infty} q_n(x) \equiv 0$  for  $x > 0$ . This is the physical solution. (See Figure 1)

Now let  $l = 0$  and  $L = 2$ . By Corollary 0.2 we cannot get an integrable potential in this case because  $|l - L| > 1$  (see Figure 1). In Refs. (A. G. Ramm, *Applic. Anal.* **81**, 833, (2002); A. G. Ramm, *Mod. Phys. Lett. B* **22**, 2217, (2008)) it has been shown explicitly that equation (1) is not uniquely solvable at some  $x$  for this case. However, while Refs. (A. G. Ramm, *Applic. Anal.* **81**, 833, (2002); A. G. Ramm, *Mod. Phys. Lett. B* **22**, 2217, (2008)) suggest that this fact makes the Cox-Thompson

scheme useless, in this paper we have shown that in order to get an integrable potential, the choice  $L = 2$  is not permitted because the set  $\Omega$  is not empty. On the other hand, Corollary 0.2 provides a one-to-one correspondence between the phase shift and the  $L$  parameter of the Cox-Thompson method at the one-term level. This correspondence has the property that the potential constructed from  $L$  belongs to  $L_{1,1}(0, \infty)$  and possesses the specified phase shift.

Applications (see Refs. B. Apagyi, Z. Harman and W. Scheid, J. Phys. A: Math. Gen. **36**, 4815, (2003), O. Melchert, W. Scheid and B. Apagyi, J. Phys. G **32**, 849, (2006), B. Apagyi W. Scheid, O. Melchert and D. Schumayer, Nuclear Physics A **790**, 767c, (2007), D. Schumayer, O. Melchert, W. Scheid and B. Apagyi, J. Phys. B: At. Mol. Opt. Phys. **41**, 035302, (2008), T. Pálmai, M. Horváth and B. Apagyi, J. Phys. A: Math. Theor. **41**, 235305, (2008), T. Pálmai, M. Horváth and B. Apagyi, Mod. Phys. Lett. B **22**, 2191, (2008)) of the Cox-Thompson scheme for  $|S| \neq 1$  suggest the existence of a connection like Corollary 0.2 that specifies one non-singular potential out of the possible infinite singular solutions. However such a theorem has, as yet, not been proven.

### 3.2 Simplified solution of the Cox-Thompson inverse scattering method at fixed energy

The Cox-Thompson method connects the  $S$ -matrix with a "reactance" matrix  $\mathcal{K}_l^\pm$  (T. Palmai, H. Horvath, B. Apagyi, J. Phys. A: Math. Theor. **41** (2008) 235305)

$$S_l = \frac{1 + i\mathcal{K}_l^+}{1 - i\mathcal{K}_l^-}, \quad l \in S, \quad (5)$$

where

$$\mathcal{K}_l^\pm = \sum_{L \in T, l' \in S} (M_{\sin})_{lL} (M_{\cos}^{-1})_{Ll'} e^{\pm i(l-l')\pi/2}, \quad l \in S,$$

and

$$\left\{ \begin{array}{c} M_{\sin} \\ M_{\cos} \end{array} \right\}_{lL} = \frac{1}{L(L+1) - l(l+1)} \left\{ \begin{array}{c} \sin \left( (l-L)\frac{\pi}{2} \right) \\ \cos \left( (l-L)\frac{\pi}{2} \right) \end{array} \right\},$$

$$l \in S, L \in T, S \cap T = \{ \}.$$

An essential simplification has been found which can be used in the cases when only even or odd partial waves contribute to the scattering. This simplifications of the equations can be used to construct different simple approximations to the Cox-Thompson-method. For example, in the scattering of  $^{12}\text{C}$  on  $^{12}\text{C}$  the elastic cross sections are generated by even partial phase shifts only.

By solving the Gel'fand-Levitan-Marchenko-type integral equation one writes the transformation kernel in the form as a sum over an artificial angular momentum space  $L \in T$ :

$$K(x, y) = \sum_{L \in T} A_L(x) u_L(y).$$

One finds for the asymptotic expansion functions  $A_L^a(x) \equiv A_L(x \rightarrow \infty)$  the relation

$$\sum_{L \in T} A_L^a(x) \frac{\cos((l-L)\frac{\pi}{2})}{l(l+1) - L(L+1)} = -\cos(x - l\frac{\pi}{2}), \quad l \in S.$$

If this equation is differentiated twice with respect to  $x$ , we obtained the following equation

$$\frac{d^2 A_L^a(x)}{dx^2} = -A_L^a(x),$$

which has the periodic solution

$$A_L^a(x) = a_L \cos(x) + b_L \sin(x).$$

Then we introduced two systems of equations for even  $l = l_e$  and odd  $l = l_o$  angular momenta as follows

$$\sum_{L \in T_e} \begin{Bmatrix} a_L \\ b_L \end{Bmatrix} \frac{\cos((l-L)\frac{\pi}{2})}{L(L+1) - l(l+1)} = \begin{Bmatrix} \cos(l\frac{\pi}{2}) \\ \sin(l\frac{\pi}{2}) \end{Bmatrix}, \quad l \in S_e$$

and

$$\sum_{L \in T_o} \begin{Bmatrix} a_L \\ b_L \end{Bmatrix} \frac{\cos((l-L)\frac{\pi}{2})}{L(L+1) - l(l+1)} = \begin{Bmatrix} \cos(l\frac{\pi}{2}) \\ \sin(l\frac{\pi}{2}) \end{Bmatrix}, \quad l \in S_o,$$

where  $|T_e| = |S_e|$ ,  $|T_o| = |S_o|$  and  $T_e \cap S_e = \emptyset$ ,  $T_o \cap S_o = \emptyset$ . These systems can be analytically solved. For even  $l$  value we obtained

$$a_L = \frac{\prod_{l \in S_e} (L(L+1) - l(l+1))}{\prod_{L' \in T_e \setminus \{L\}} (L(L+1) - L'(L'+1))} \frac{1}{\cos\left(\frac{L\pi}{2}\right)}, \quad b_L = 0, \quad L \in T_e,$$

and similarly for odd orbital angular momenta  $l_o \in S_o$ . Now by using these analytical expressions one obtains the final solution to the CT method for even  $l$  as:

$$\tan(\delta_l) = - \sum_{L \in T_e} \frac{\prod_{l' \in S_e \setminus \{l\}} (L(L+1) - l'(l'+1))}{\prod_{L' \in T_e \setminus \{L\}} (L(L+1) - L'(L'+1))} \tan\left(\frac{L\pi}{2}\right), \quad l \in S_e. \quad (6)$$

A similar relation is obtained for odd orbital angular momenta  $l_o \in S_o$ . The above equations determine the unknown set  $T_e$  of shifted angular momenta  $L$ . These equations are much simpler to solve as the above equations which contain the inversion of the matrix of  $M_{\cos}$  involving the unknowns of shifted angular momenta  $L$ . We showed that the solutions with even  $l = l_e$  of equations (6) are equivalent to the solution of equation (5) with input phase shifts to even  $l$  values.

There are several approximations possible with this simplified method. One can solve the inverse potential for the sets  $T_e$  and  $T_o$  and obtains the potentials  $q_e$  and  $q_o$ . We simply added them together to get an approximation of the interaction potential  $q_A(x) = q_e(x) + q_o(x)$ . This is called the potential approximation  $A$ . One may try to approximate the set of the shifted angular momenta themselves by solving the equations for even and odd phase shifts separately, obtaining the sets  $T_e$  and  $T_o$ . One gets the  $T$ -set approximation  $T_a = T_e \cup T_o$  and then the approximate potential  $q_T(x)$ . If the collision is dominated by a single partial wave as in the case of resonance scattering then the equations can be solved for  $N = 1$ , and this results in the simple expression  $L = l - 2\delta_l/\pi$  for the shifted angular momentum (approximation  $L$ ). This approximation used for all shifted angular momenta yields an inverted potential denoted by  $q_L(x)$ .

We applied the new method to calculate an effective  $^{87}\text{Rb}+^{87}\text{Rb}$ -potential observed in ultracold Bose-gas collision at an energy of  $E = 303\mu\text{K}$ . The inverse calculation uses only even measured phase shifts with angular momenta  $l = 0, 2, 4$ , respectively. The resulting potential shown in Fig. 2 is

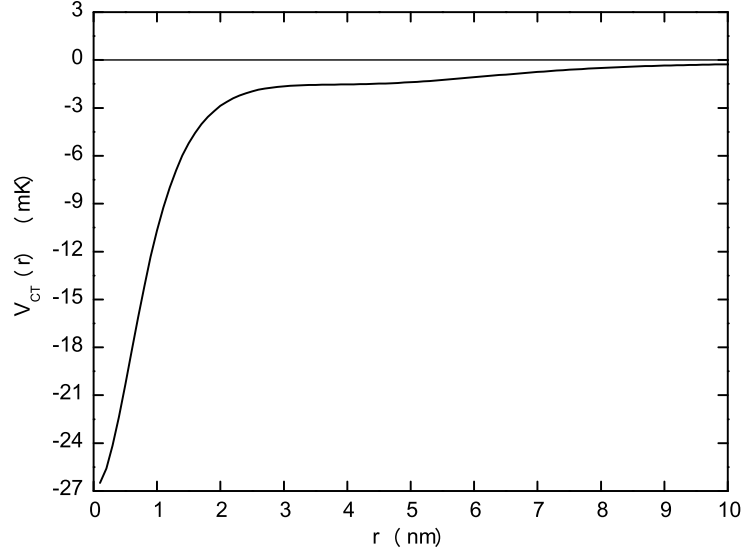


Figure 2: Effective  $^{87}\text{Rb}+^{87}\text{Rb}$  inverse potential  $V_{\text{CT}}$  (in mK) as a function of the radial distance  $r$  (in nm) at an energy  $E_{cm} = 303 \mu\text{K}$ .

identical with the potential obtained by solving the complete set of equations (see chapter 3.3).

We calculated also the inverse potential for the  $n+^{12}\text{C}$  scattering at  $E_{lab} = 10 \text{ MeV}$  with complex-value phase shifts derived by Chen and Thornow from experimental cross sections. The inverse potentials are obtained with different approximations. It is assumed that the potential calculated by the original CT-method would be the best one. In Fig. 3 we show inverse potentials obtained with the approximations A,T, and L.

The range of applicability of the new formulas is wider than the original Cox-Thompson method. We have demonstrated the applicability of the new equations which make the solution of the CT inverse scattering method at fixed energy much easier.

### 3.3 The effective Rb-Rb interatomic potential from ultracold Bose-Einstein gas collisions

At very low energies, one can cool down atoms to the ultracold regime ( $< 1 \mu\text{K}$ ), to form a Bose-Einstein condensate and explore the low-energy

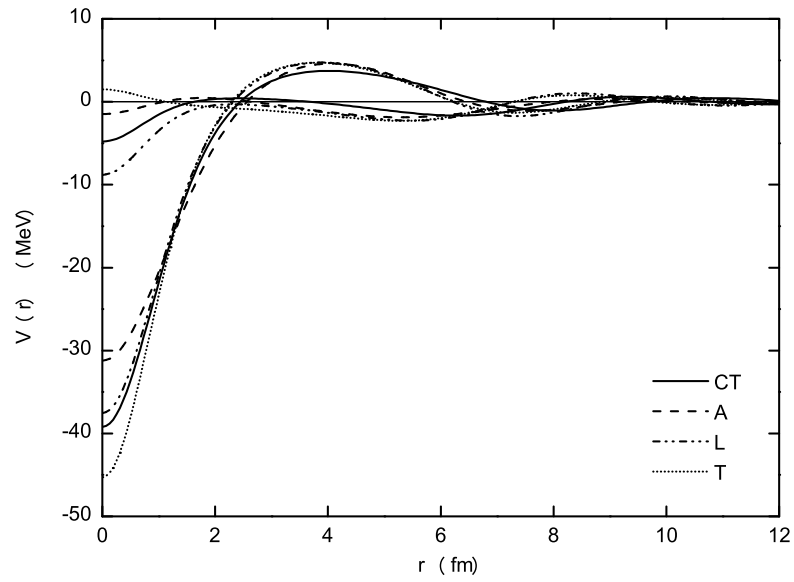


Figure 3: Inverse potentials obtained from input phase shifts up to  $l = 4$  for  $n$  scattering on  $^{12}\text{C}$  at an energy  $E_n^{\text{lab}} = 10$  MeV ( $E_n^{\text{c.m.}} = 9.23$  MeV,  $k = 0.638$  fm $^{-1}$ ). Curves obtained by the CT and by the approximate methods are labeled according to the procedure discussed in the text. The four curves around  $V \approx 0$  are the imaginary parts of the potentials.

properties of the atomic interaction. At these temperatures collisions play a major role in affecting the static and dynamic properties of the condensate, e.g. stability, lifetime, and thermalization rate. In this regime inelastic processes are usually negligible. Here, we characterized or reconstructed an effective inter-atomic potential from scattering phase shifts by using the inverse scattering method and by assuming that there exists an effective spherically symmetric potential which causes the observed scattering events (D. Schumayer, O. Melchert, W. Scheid, B. Apagyi, J. Phys. B: At. Mol. Opt. Phys. **41** (2008) 035302).

We employed the fixed energy inverse scattering method of Cox and Thompson (CT) in order to derive model-independent potentials from given phase shifts resulting from experiments with a Rb-Bose-Einstein gas in traps. The CT method leads to a system of nonlinear equations

$$\exp(2i\delta_l) = \frac{1 + i\mathcal{K}_l^+}{1 - i\mathcal{K}_l^-},$$

where the reactance matrix is defined as

$$\mathcal{K}_l^\pm = \sum_{L \in T, l' \in S} \mathcal{N}_{lL} (\mathcal{M}^{-1})_{Ll'} e^{\pm i(l-l')\pi/2}, \quad l \in S$$

with the square matrices

$$\begin{aligned} \left\{ \begin{array}{c} \mathcal{N} \\ \mathcal{M} \end{array} \right\}_{lL} &= \frac{1}{L(L+1) - l(l+1)} \left\{ \begin{array}{c} \sin((l-L)\pi/2) \\ \cos((l-L)\pi/2) \end{array} \right\}, \\ l \in S, L \in T, S \cap T &= \{ \}, \end{aligned}$$

containing the unknown  $L$ -values. Once the set  $T$  is determined by solving the highly nonlinear equations given above for  $L$ , we calculated the coefficient functions  $A_L(r)$  using the system of linear equations

$$\sum_{L \in T} A_L(r) (j_L(r) \times n'_l(r) - j'_L(r) \times n_l(r)) / [l(l+1) - L(L+1)] = n_l(r),$$

where  $j_L$  and  $n_l$  denote spherical Bessel and Neumann functions. Next, we calculated the potential with the expansion coefficients  $A_L(r)$

$$V(r) = -\frac{2}{r} \frac{d}{dr} \sum_{L \in T} A_L(r) j_L(r) / r.$$

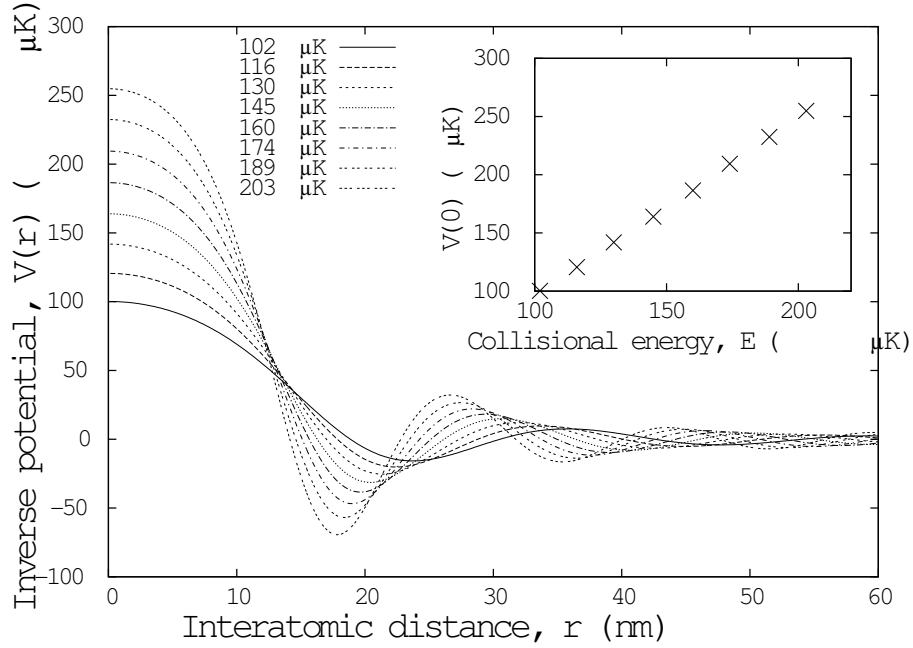


Figure 4: Inverse potentials from the  $l = 0, 2, 4$  experimental phase shifts at energies  $E=102-203 \mu\text{K}$  below the  $d$ -resonance. The inset shows the inverse potential  $V(r = 0)$  at  $r = 0$  as a function of collision energy.

In Fig. 4 we present the inversion potentials for the energy range between 100 and 200  $\mu\text{K}$  which lie below the characteristic  $l = 2$  resonance of  $^{87}\text{Rb}$ - $^{87}\text{Rb}$  scattering at  $\sim 275 \mu\text{K}$ . The inversion potentials reproduce the input phase shifts well within the considered energy region as demonstrated in Fig. 5 where both input and output phase shifts are shown. Fig. 6 gives the inversion potentials from 200 to 400  $\mu\text{K}$ . There occurs an abrupt change of the potential strength  $V(0)$  at  $r = 0$  from repulsion to attraction when the collision energy crosses the  $l = 2$  resonance at  $\sim 275 \mu\text{K}$ .

Since the input data stem entirely from experimentally confirmed data we expect that the sudden change of the inner strength of the potential should be observed in future Bose-Einstein gas experiments. This inversion technique is useful if high-resolution data are available. The corresponding potential has not already been studied with models, especially if one needs an intuitive picture about the interaction in a given energy range.

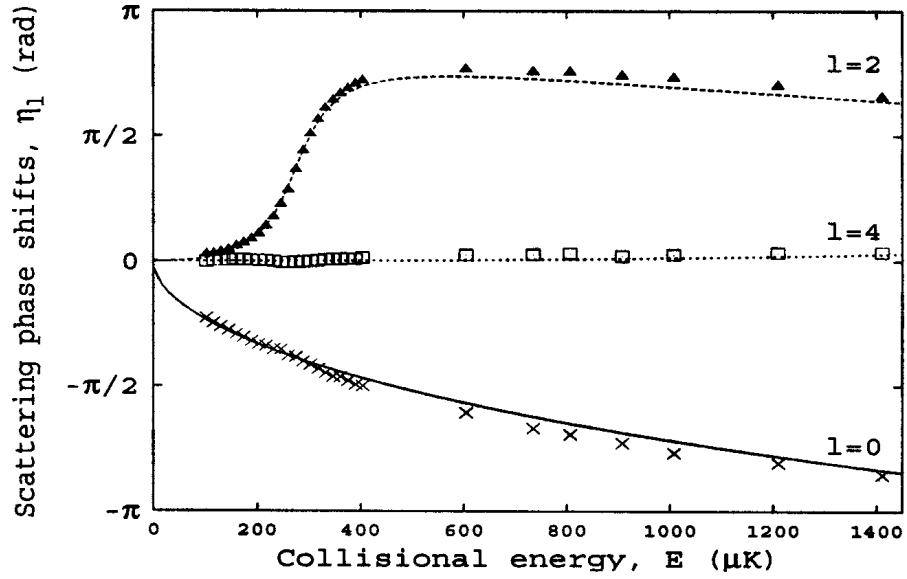


Figure 5: Phase shifts of the first three allowed partial waves with  $l = 0, 2, 4$ . Solid and dashed lines represent the original input data. The symbols stand for phase shifts calculated from the inverse potentials shown in Figs 6 and 8.

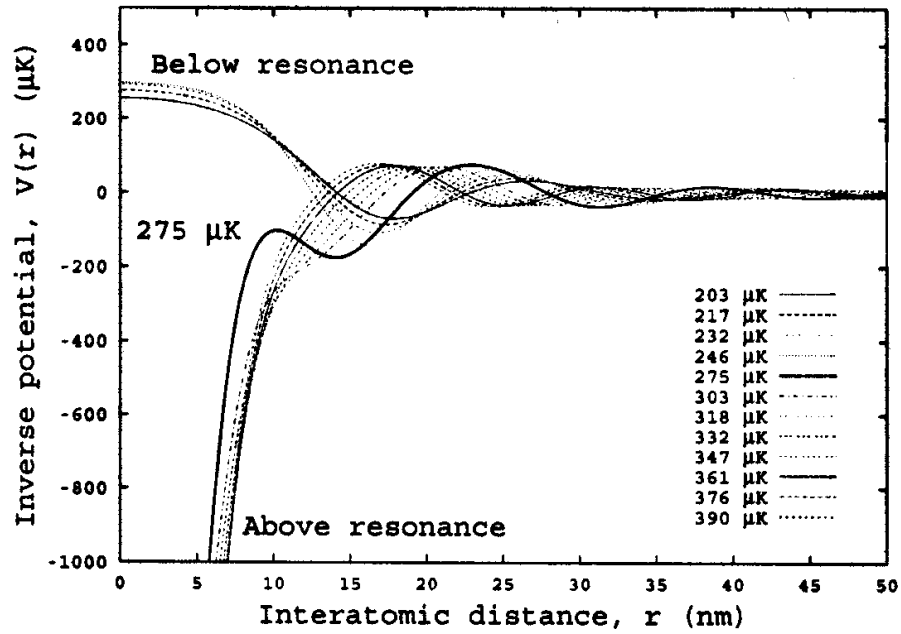


Figure 6: Inverse potentials obtained from the experimental  $l = 0, 2, 4$  scattering phase shifts around the  $d$ -resonance at  $\sim 275 \mu\text{K}$ .

### 3.4 Stability of static solitonic excitations of two-component Bose-Einstein condensates in the finite range of interspecies scattering lengths

Over the past few years an increasing interest could be observed in the case of atomic Bose-Einstein condensates (BECs). Mostly one-component BECs have been studied so far for the elements  $^1\text{H}$ ,  $^7\text{Li}$ ,  $^{23}\text{Na}$ ,  $^{41}\text{K}$ ,  $^{85,87}\text{Rb}$ , and  $^{133}\text{Cs}$ . The two-component systems Na-Rb and K-Rb have been considered theoretically and the mixture Cs-Li has been investigated experimentally, without reaching the BEC phase. In this project we found a simple treatment of the stability of a condensate mixture consisting of two atomic species (D. Schumayer, B. Apagyi, Phys. Rev. A **69** (2004) 043620).

For treating two interacting dilute Bose-Einstein condensates we started with the zero temperature mean field theory neglecting collisions between the condensed atoms and the thermal cloud. The macroscopic dynamics in such a physical condensate is described by two coupled nonlinear Schrödinger equations (NLSs). These equations are also known as Gross-Pitaevskii (GP) equations. Restricting ourselves to (1 + 1) dimensions the coupled GP equations can be written as follows ( $i, j = 1, 2$ )

$$i\hbar\frac{\partial\psi_i}{\partial t} = \left[ -\frac{\hbar^2}{2m_i}\frac{\partial^2}{\partial x^2} + \sum_{j=1}^2\Omega_{ij}|\psi_j|^2 + V_i \right] \psi_i, \quad (12)$$

where  $m_i$  denotes the individual mass of the  $i$ th atomic species,  $\Omega_{ij} = 2\pi\hbar^2 a_{ij}/A\mu_{ij}$  with  $a_{ij}$  being the 3-dimensional scattering length between atoms of species  $i, j$ , respectively,  $A$  the general transverse crossing area of the cigar-shape BEC,  $\mu_{ij} = m_i m_j / (m_i + m_j)$  the reduced mass, and  $V_i$ , ( $i = 1, 2$ ) in Eq (12) are the external trapping potentials. The normalization of the wave functions is given by  $N_i = \int_{-\infty}^{\infty} |\psi_i|^2 dx$ , for  $i = 1$  and 2 with  $N_i$  denoting the number of the individual atoms in the  $i^{\text{th}}$  component of the BEC.

The stationary solutions of the coupled GP equations (12) are taken in the form  $\psi_i(x, t) = \Phi_i(x) \exp(-iE_i t/\hbar)$  where  $E_i$  is the single-particle energy of the  $i^{\text{th}}$  component. With this wave function and neglecting the kinetic terms in (12) we derived approximate density profiles and a semi-infinite

range for the scattering length  $a_{ij}$  between two different atoms. From the GP equations (12) we obtained the so called Thomas-Fermi approximation

$$|\Phi_1(x)|^2 = \frac{\Omega_{22}(E_1 - V_1(x)) - \Omega_{12}(E_2 - V_2(x))}{\Delta},$$

$$|\Phi_2(x)|^2 = \frac{\Omega_{22}(E_2 - V_2(x)) - \Omega_{21}(E_1 - V_1(x))}{\Delta}$$

with  $\Delta = \Omega_{11}\Omega_{22} - \Omega_{12}\Omega_{21}$ . With a harmonic external potential  $V_i(x) = \frac{1}{2}m_i\omega_i^2x^2$  ( $i = 1, 2$ ) one can write ( $i = 1, 2$ )

$$|\Phi_i(x)|^2 = A_i(x_i^2 - x^2)/\Delta \quad \text{if } |x| \leq x_i, \quad i = 1, 2,$$

$$|\Phi_i(x)|^2 = 0 \quad \text{if } |x| > x_i, \quad i = 1, 2.$$

The constants are  $A_i = (\Omega_{jj}m_i\omega_i^2 - \Omega_{ij}m_j\omega_j^2)/2$  and  $x_i = \pm(3\Delta N_i/4A_i)^{1/3}$  obtained from the normalization condition  $\int_{-x_i}^{x_i} |\Phi_i(x)|^2 dx = N_i$  ( $i = 1, 2$ ). The excited static solutions have the form ( $i = 1, 2$ )

$$\tilde{\psi}_i(x, t) = \Phi_i(x)\phi_i(x) \exp(-i\tilde{E}_i t/\hbar)$$

with  $\phi_i(x)$  being an excess or defect of the  $i^{th}$  component of the background density. Inserting this ansatz into the GP equations (12) and assuming that the excitation mechanism is restricted to a small interval  $x \in (-L_i, L_i)$  around  $x = 0$ , one obtains two coupled equations for the perturbing functions

$$\tilde{E}_1\phi_1 = -\frac{\hbar^2}{2m_1}\frac{\partial^2\phi_1}{\partial x^2} + \tilde{\Omega}_{11}|\phi_1|^2\phi_1 + \tilde{\Omega}_{12}|\phi_2|^2\phi_1 \quad (13a)$$

$$\tilde{E}_2\phi_2 = -\frac{\hbar^2}{2m_2}\frac{\partial^2\phi_2}{\partial x^2} + \tilde{\Omega}_{21}|\phi_1|^2\phi_2 + \tilde{\Omega}_{22}|\phi_2|^2\phi_2 \quad (13b)$$

with  $\tilde{\Omega}_{ij} = \Omega_{ij}A_jx_j^2/\Delta$  ( $i, j = 1, 2$ ). Very small potential terms have been neglected. These equations determine the perturbing functions  $\phi_i(x)$  within the range  $|x| \leq L_i < x_i$ . Since static one-soliton solution of the B or the D type can be produced in BECs we tried to use static uncoupled soliton solutions

$$\phi_{B1}(x) = q_1 \text{sech}(k_1x)$$

$$\phi_{D2}(x) = q_2 \tanh(k_2x)$$

with complex amplitudes  $q_i$  and range parameters  $k_i \sim L_i^{-1}$  for the description of the excitation of the two-component BECs. In accordance

with the soliton characters we imposed the appropriate boundary conditions  $\phi_{B1}(x \rightarrow \pm\infty) = 0$ , and  $\phi_{D2}(x \rightarrow \pm\infty) = \pm q_2$ .

The insertion of the above solitonic ansatz into the equations (13) gives  $k_1 = k_2 \equiv k$  for the range parameters and the relations

$$|q_1|^2 = \frac{\hbar^2 k^2}{\Delta} \left( \frac{\tilde{\Omega}_{12}}{m_2} - \frac{\tilde{\Omega}_{22}}{m_1} \right),$$

$$|q_2|^2 = \frac{\hbar^2 k^2}{\Delta} \left( \frac{\tilde{\Omega}_{11}}{m_2} - \frac{\tilde{\Omega}_{21}}{m_1} \right)$$

for the modulus of the amplitudes.

The requirement that the modulus of the two amplitudes  $q_1$  and  $q_2$  is positive and real yields the following stability conditions ( $A_{ij} = a_{ij}(1 + m_i/m_j)$ )

$$f_{B1}(a_{12}) = \frac{A_{12} - A_{22}}{\det(A)} \geq 0, \quad (14a)$$

$$f_{D2}(a_{12}) = \frac{A_{11} - A_{21}}{\det(A)} \geq 0 \quad (14b)$$

for the existence of B and D solitonic excitations within the two component BEC. Although the above conditions are independent of the particle numbers  $N_i$ , one has a constraint by the particle number conservation because the normalization of the B and D solitonic excitation reads as

$$N_1 = 2|q_1|^2 \frac{A_1}{\Delta} n(kx_1),$$

$$N_2 = 2|q_2|^2 \frac{A_2}{\Delta} \left( \frac{2}{3}(kx_2)^2 - n(kx_2) \right),$$

with  $n(w) = -w^2 + 2w \ln[1 + \exp(2w)] + \text{dilog}[1 + \exp(2w)] + \frac{\pi^2}{12}$ .

Assuming now that the system parameters  $m_1$ ,  $m_2$ ,  $a_{11}$  and  $a_{22}$  are given, and disregarding the particle numbers  $N_i$ , we determined the broadest range of the interspecies scattering length  $a_{12}$  for which the existence of solitons in the two-component BEC can be expected. If the actual value of  $a_{12}$  was determined then we found the particle number ratio  $N_2/N_1$  or the size parameter  $k$  in order to get information about the two-component system which can show static solitonic features.

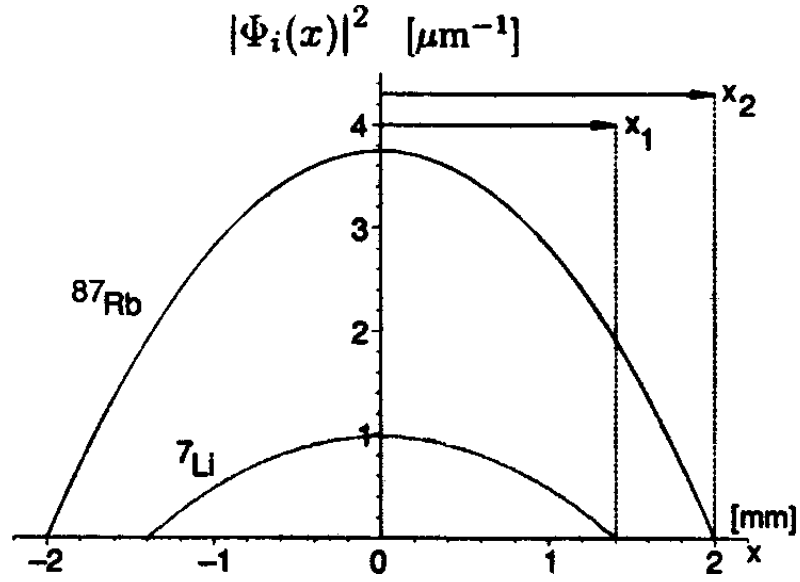


Figure 7: The density profile  $|\Phi_i|^2$  of the Thomas-Fermi approximation for a two-component BEC, namely for the mixture  ${}^7\text{Li} - {}^{87}\text{Rb}$ , with parameters  $a_{11} = -1.4$  nm ( ${}^7\text{Li}$ ),  $a_{22} = 5.5$  nm ( ${}^{87}\text{Rb}$ ) and  $a_{12} = 4.5$  nm.

In Fig.7 we show the density profile  $|\Phi_i|^2$  of the Thomas-Fermi approximation for a two-component BEC, namely for the mixture  ${}^7\text{Li} - {}^{87}\text{Rb}$ , with parameters  $a_{11} = -1.4$  nm ( ${}^7\text{Li}$ ),  $a_{22} = 5.5$  nm ( ${}^{87}\text{Rb}$ ) and the chosen interspecies scattering length  $a_{12} = 4.5$  nm.

3.5 Evolution solution (simulation) of the nonlinear Schrödinger equation  
Our aim is to solve the evolution problem of the Gross-Pitaevskii (GP) equation (which is a nonlinear Schrödinger (nls) equation with external potential  $V$ )

$$iu_t = -HV u_{xx} + C |u|^2 u + Vu, \quad u = u(x, t), \quad V = V(x) \quad (15)$$

with a given initial condition  $u_0(x) = u(x, 0)$ . In the case of special values of the constants  $HV$  and  $C$ , and for zero potential  $V = 0$  there are some exact solutions to the equation known also as a nonlinear Schrödinger (nls) equation.

$$iu_t = -HV u_{xx} + C |u|^2 u, \quad u = u(x, t). \quad (15a)$$

Colliding two-soliton solution

Let us consider the following nls equation

$$iu_t = u_{xx} + 2|u|^2u \quad (16)$$

which means that we use  $HV = -1$ ,  $C = +2$  and  $V = 0$  in (15). Equation (16) admits the following (colliding) two-soliton solution:

$$u(x, t) = \frac{e^{-i(2x-20-3t)}}{\cosh(x-10-4t)} + \frac{e^{+i(2x+20-3t)}}{\cosh(x+10+4t)} \quad (17)$$

### Bright soliton solution

The most widely known soliton solution of the nls equation of the form

$$iu_t = -u_{xx} - |u|^2u \quad (HV = 1, C = -1, V = 0) \quad (18)$$

is the bright soliton. Its general form is the following:

$$u(x, t; a, c) = a e^{i(\frac{c}{2}(x-ct)+nt)} / \cosh(a(x-ct)/\sqrt{2}) \quad (19)$$

with the constraint  $a^2 = 2(n - (\frac{c}{2})^2) > 0$ .

If  $c = 1$ ,  $n > \frac{1}{4}$ . Let  $n = \frac{5}{4}$ . Then  $a^2 = 2$ ,  $a = \sqrt{2}$ . The bright soliton solution is then

$$u(x, t; \sqrt{2}, 1) = \sqrt{2}e^{i(\frac{1}{2}(x-t)+\frac{5}{4}t)} / \cosh(x-t). \quad (20)$$

The initial condition in this case is

$$u(x, 0; \sqrt{2}, 1) = \sqrt{2}e^{ix/2} / \cosh(x) \quad (21a)$$

and the norm is (independent of  $t$ ):

$$\int |u(x, t; \sqrt{2}, 1)|^2 dx = 4. \quad (21b)$$

In case of  $c = 2$  we have the bright soliton

$$u(x, t; \pm 2, 2) = \pm 2e^{i((x-2t)+3t)} / \cosh(\pm\sqrt{2}(x-2t)), \quad (22)$$

and the initial condition

$$u(x, 0; \pm 2, 2) = \pm 2e^{ix} / \cosh(\pm\sqrt{2}x). \quad (22a)$$

### Dark soliton solution

The nls equation

$$iu_t = -u_{xx} + |u|^2u \quad (HV = 1, C = +1, V = 0) \quad (23)$$

supports dark soliton solution of the form

$$u(x, t; m, c) = re^{i(\Theta - mt)}, \quad (23a)$$

with real amplitude  $r = r(x - ct)$ , real phase  $\Theta = \Theta(x - ct)$ , and real parameters  $c = \text{const}$ ,  $m = \text{const} > c^2/2 > 0$  satisfying the relations

$$r^2 = m - 2\kappa^2 / \cosh^2(\kappa(x - ct))$$

and

$$1/\tan(\Theta) = -2\kappa \tanh(\kappa(x - ct)).$$

In the course of testing the simulation program we shall use the dark soliton solution with parameters  $m = 1, c = 1$ .

#### Ma solitary wave solution

Equation

$$iu_t = -u_{xx} - |u|^2u \quad (HV = 1, C = -1, V = 0) \quad (24)$$

also has the Ma solitary wave solution of the form

$$u(x, t; a, m) = ae^{ia^2t} [1 + 2m(m \cos \Theta + in \sin \Theta) / f(x, t)] \quad (25)$$

with real parameters  $a$  and  $m$  and the following relations and definitions:

$$n^2 = 1 + m^2, \quad \Theta = 2mna^2t, \quad f(x, t) = n \cosh(ma\sqrt{2}x) + \cos \Theta.$$

In the course of testing the simulation program we shall use the Ma solitary wave solution with parameters  $a = 1, m = 1/2$ .

#### Rational-cum-oscillatory solution

Equation

$$iu_t = -u_{xx} - |u|^2u \quad (HV = 1, C = -1, V = 0) \quad (26)$$

also has the rational-cum-oscillatory solution of the form

$$u(x, t) = e^{it} \left[ 1 - \frac{4(1 + 2it)}{1 + 2x^2 + 4t^2} \right] \quad (27).$$

#### Simulation procedure

To solve the time evolution problem of the Schrödinger equation

$$iu_t(x, t) = Hu(x, t), \quad u(x, t) = e^{-iHt}u(x, t) \quad (28)$$

one discretises eq. (28) in time ( $t_n = n\tau$  ( $n = 0, 1, \dots, NT$ )), and space, ( $x_j = jh$  ( $j = 1, 2, \dots, N$ )), and denotes the wave function by  $u_j^n \equiv u(x_j, t_n)$ .

One makes use of the basic relation that the backward and forward time evolutions at  $t_{n+1/2}$  result in the same value of the wave function at every point  $x_j$ , that is

$$u_j^{n+1/2} = (1 + \frac{1}{2}iH\tau)u_j^{n+1} = (1 - \frac{1}{2}iH\tau)u_j^n = u_j^{n+1/2} \quad (29)$$

or, using instead of  $1/2$  the symbol  $\sigma$ ,

$$u_j^{n+\sigma} = (1 + \sigma iH\tau)u_j^{n+1} = (1 - \sigma iH\tau)u_j^n = u_j^{n+\sigma}, \quad (29a)$$

The Crank-Nicholson scheme corresponds to  $\sigma = 1/2$ .

By re-ordering equation (29a) one gets the basic formula:

$$iu_j^{n+1} - \tau H\sigma u_j^{n+1} = iu_j^n + \tau(1 - \sigma)Hu_j^n \quad (30)$$

with the Hamiltonian acting at point  $x_j$  on the wave function  $u_j$  as

$$Hu_j = -\frac{HV}{h^2}(u_{j+1} - 2u_j + u_{j-1}) + V_j u_j$$

with  $V_j = V(x_j) + C|u_j|^2$ . By using this form, eq.(30) can be written into a form

$$T^{(n)}u^{n+1} = F^n \quad (31)$$

where  $T^{(n)}$  denotes an  $N \times N$  triangular matrix with elements  $T_{j,j}^{(n)} = B_j^{(n)} = ih^2 - \tau\sigma(2HV + h^2V_j)$ ,  $T_{j+1,j}^{(n)} = T_{j,j+1}^{(n)} = A = \tau\sigma HV$  and  $F^n$  stands for an  $1 \times N$  vector whose elements are defined by  $F_j^n = C_j^n u_j^n - D(u_{j+1}^n + u_{j-1}^n)$  with  $C_j^{(n)} = ih^2 + \tau(1 - \sigma)(2HV + h^2V_j)$  and  $D = \tau(1 - \sigma)HV$ .

We use Neumann boundary condition  $u_x = 0$  at the boundaries. At the boundary the formula (30) provides the relation

$$u_j^{n+1} = \frac{i + \tau(1 - \sigma)V_j}{i - \tau(1 - \sigma)V_j}u_j^n, \quad i = 1, N. \quad (32)$$

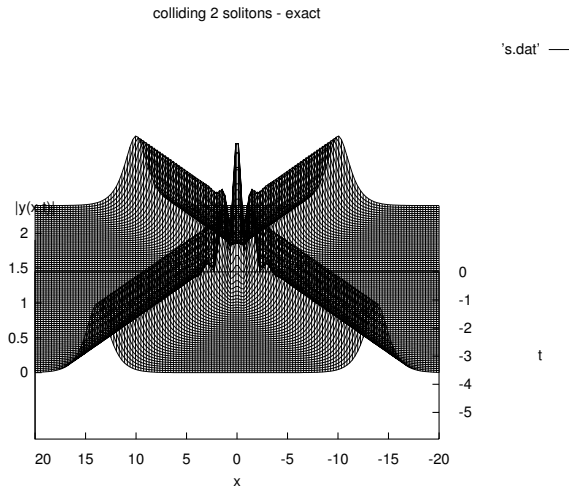


Figure 8: Colliding solitons - exact case (see eq.(17)).

Application for the one-component case:

Exact solutions, simulations and outraying

In the following figures 8-17 we studied some exact soliton solutions of the nls and their numerical simulation during the time development. Differences between exact and simulated cases cannot be observed. By starting with  $y(x, 0)$ , which does not correspond to an exact solution, the 'rest' is outraying and only the stable soliton configuration remains (see figures 18-19). One can also confine a standing wave packet inside a volume bordered by potential gates and recognize the time development of the matter (figure 20).

Applications for the two-component case:

Exact solutions, simulations and outraying

The numerical technique exhibited before can be applied also to solve coupled Gross-Pitaevskii equations. In this case the driving matrix  $T$  in eq. (31) is not a  $N \times N$  triadiagonal matrix but becomes a  $2N \times 2N$  five-band matrix whose inversion cannot be performed analytically. In this case we also performed carefully numerical tests for known examples of coupled bright-dark soliton pairs. In figure 21 the outraying process can be observed from two perspectives. The two-component mixture outrays the rest of materials and only the two bright solitons are kept being stable in time evolution.

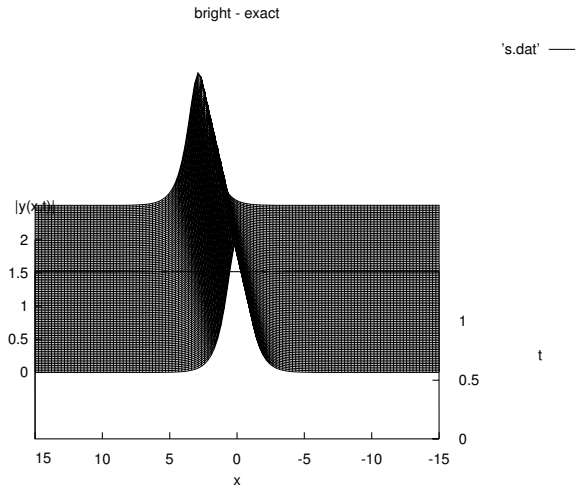


Figure 9: Bright soliton - exact case (see eq.(19)).

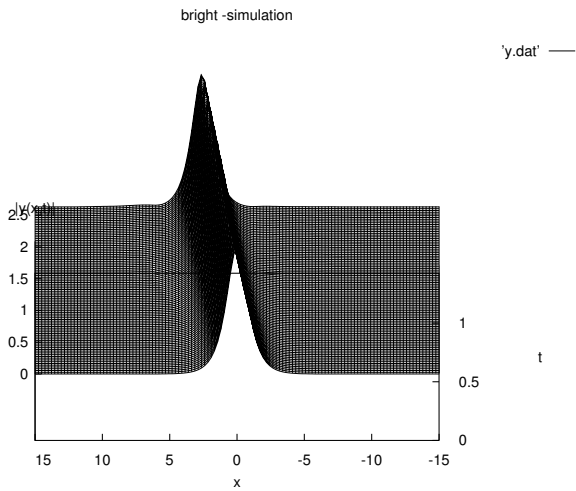


Figure 10: Bright soliton - simulation (see eq.(31)).

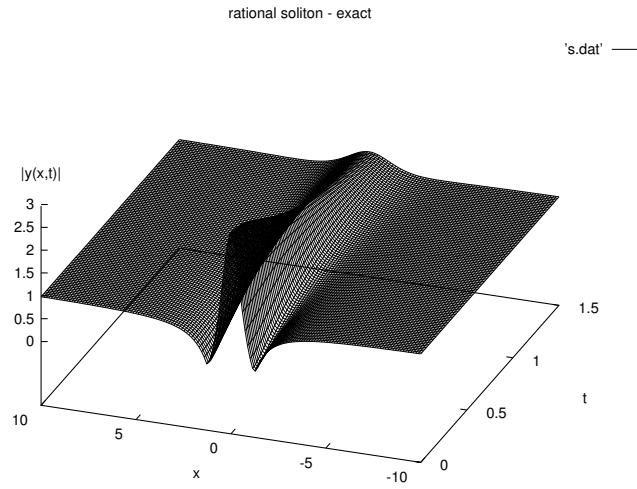


Figure 11: Bright soliton - exact case (see eq.(22)).

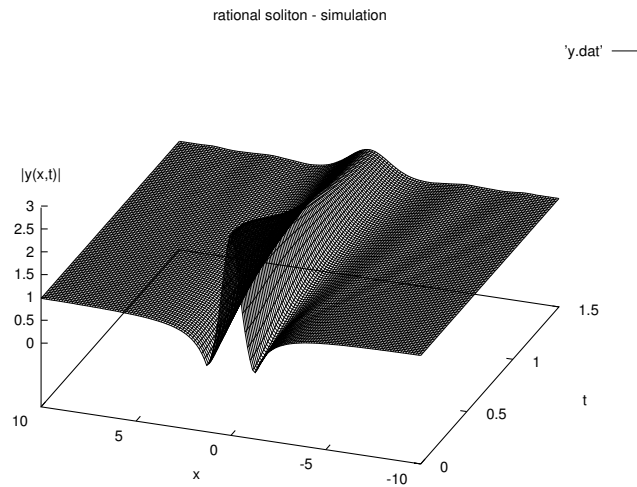


Figure 12: Bright soliton - simulation (see eq.(31)).

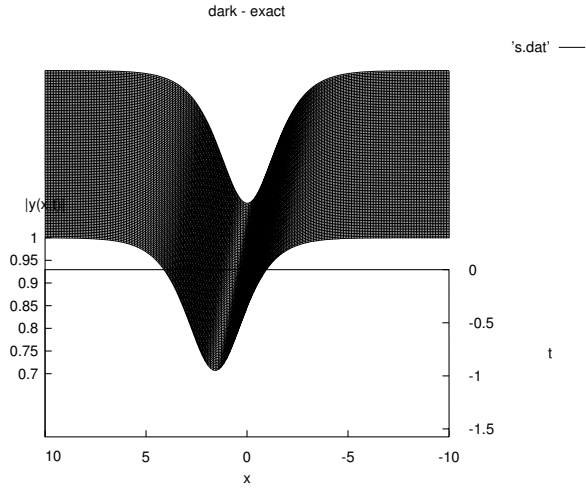


Figure 13: Dark soliton - exact case (see eq.(23a)).

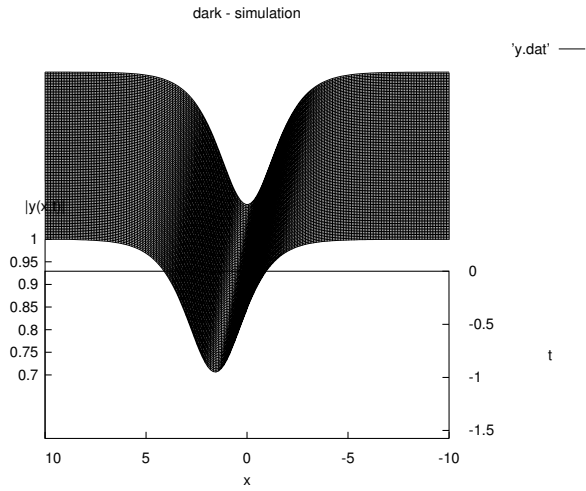


Figure 14: Dark soliton - simulation (see eq.(31)).

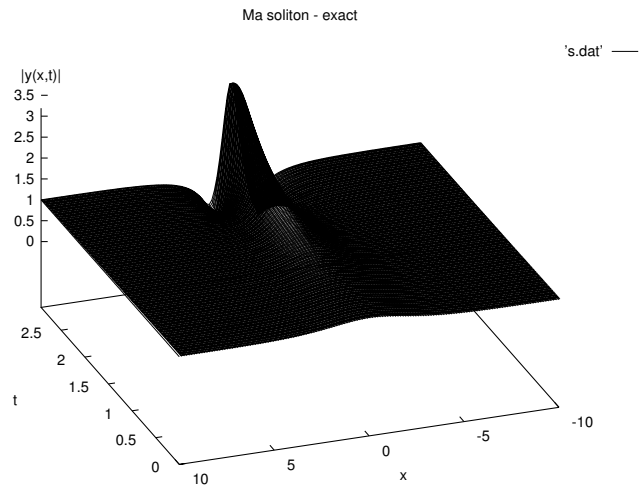


Figure 15: Ma solitary wave - exact case (see eq.(25)).

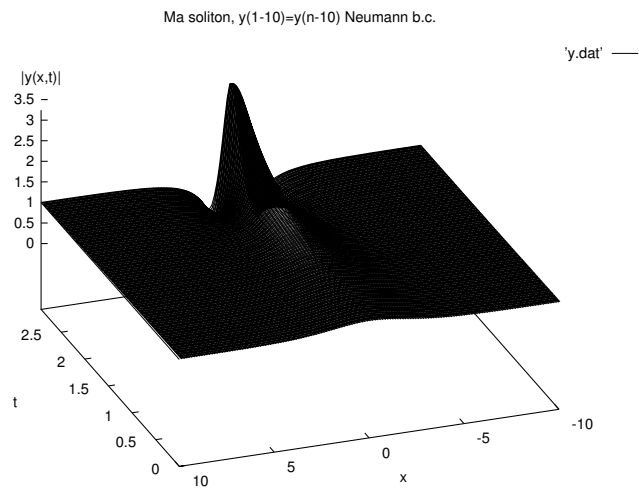


Figure 16: Ma solitary wave - simulation. Neumann b.c. used at  $j=1-10$  and  $N-10 - N$ . (see eq.(32)).

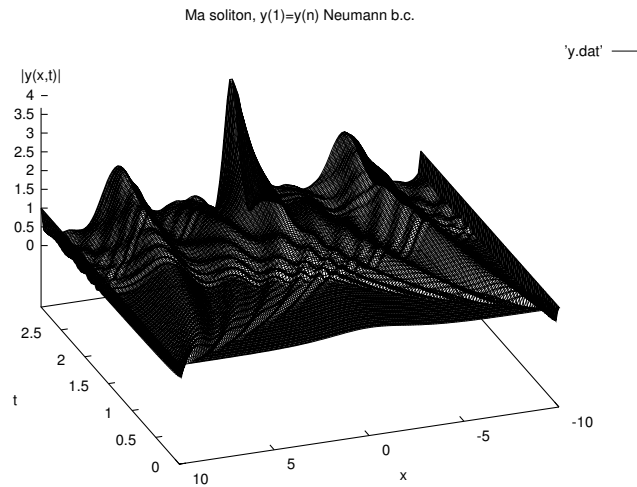


Figure 17: Ma solitary wave - simulation. Neumann b.c. used at  $j=1$  and  $N$ . (see eq.(32)).

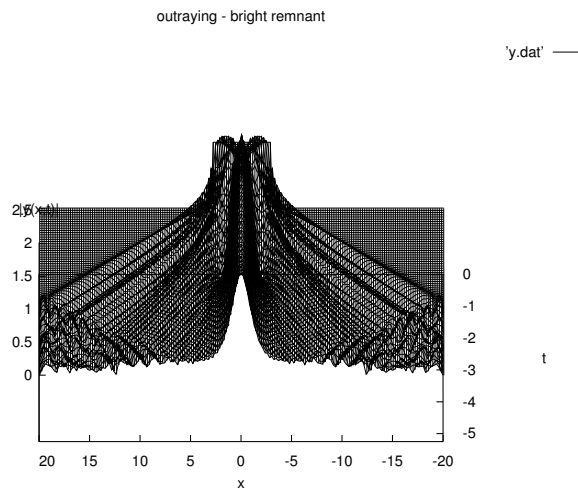


Figure 18: By starting with initial condition  $y(x, 0)$  which does not correspond to an exact solution the 'rest' is outraying and only the stable soliton configuration remains. Here is shown one soliton.

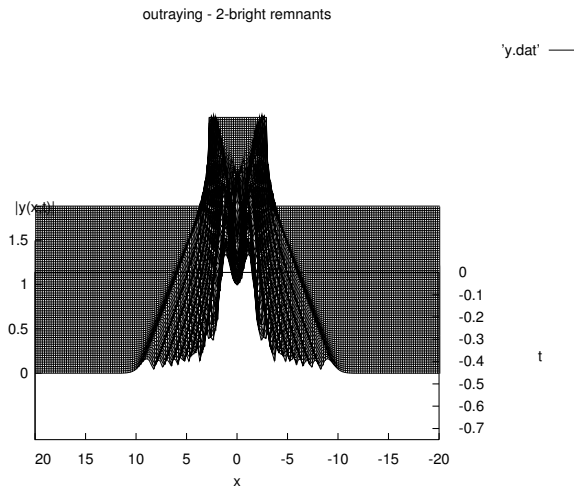


Figure 19: By starting with initial condition  $y(x, 0)$  which does not correspond to an exact solution the 'rest' is outraying and only the stable soliton configuration remains. Here are shown two solitons.

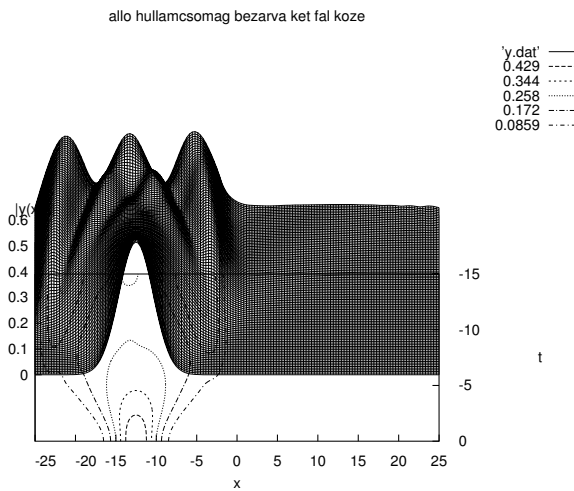


Figure 20: Development of a standing wave packet within a closed interval of space bordered by potential walls at  $x = -25$  and  $x = 0$  (not shown)

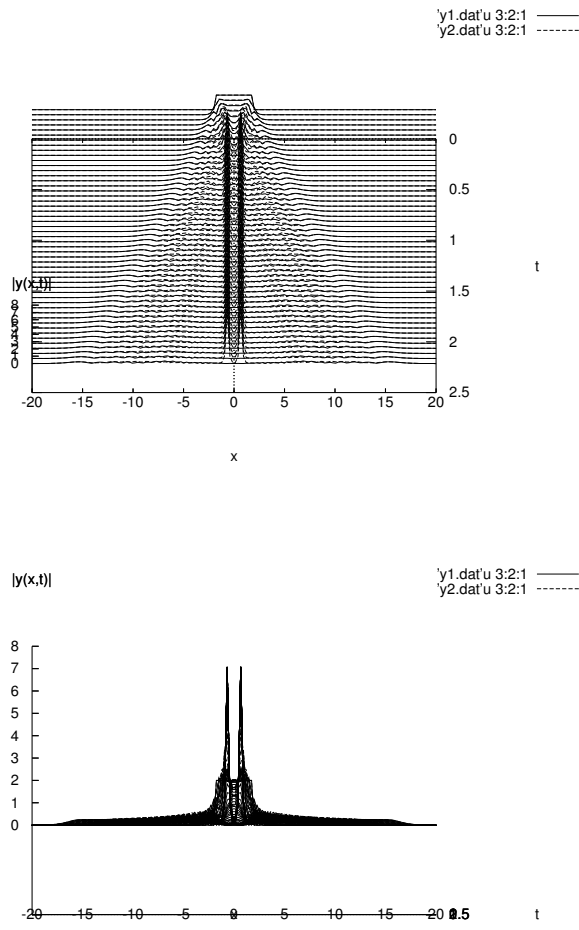


Figure 21: Outraying when a two-component mixture starts from a uniform density. Two stable solitons remain, the rest is outrayed . The process is exhibited from two perspectives.